A Fast Optimization Method for High-Speed Link Inverse Design With SVR-AS Algorithm

Hanzhi Ma[®], *Graduate Student Member, IEEE*, Da Li[®], *Member, IEEE*, Er-Ping Li[®], *Fellow, IEEE*, Andreas C. Cangellaris, *Life Fellow, IEEE*, and Xu Chen[®], *Member, IEEE*

Abstract—A fast constrained design optimization technique is introduced for the inverse design of high-speed links. The proposed method makes use of the support-vector-regression-based active subspace (SVR-AS) method to generate a lower dimensional space of active variables as a linear weighted combination of the higher dimensional design space to help simplify the optimization problem. This newly developed technique successfully transforms the complex nonlinear constraint optimization problem into a linear constraint minimization problem and provides a directly solvable function for the optimal results associated with each active variable. Furthermore, the proposed optimization algorithm can be utilized for the optimization problem with equality and inequality constraints, which contain one- and multidimensional active variables generated from the SVR-AS method. Studies of two high-speed links with channel design parameters for nonreturn-to-zero pulse and IBIS-AMI equalization settings for four-level pulse amplitude modulation, respectively, are utilized to verify the efficiency of the method. The sensitivity analysis ability of the SVR-AS method is also presented for both the one- and multidimensional active variable cases.

Index Terms—Design optimization, eye diagram, high-speed link, signal integrity.

I. INTRODUCTION

The speed and quantity of data transmission in a high-speed system have increased significantly in recent years, accompanied by increasingly serious signal integrity issues in the electronic system, which directly or indirectly affect the signal reception of the link, the quality of signal transmission, and the bit error rate. As a result, accurately characterizing and effectively analyzing signal integrity problems in high-speed

Manuscript received November 16, 2021; revised February 18, 2022 and March 28, 2022; accepted April 19, 2022. Date of publication May 10, 2022; date of current version June 13, 2022. The work of Hanzhi Ma, Da Li, and Er-Ping Li was supported in part by the National Natural Science Foundation of China under Grants 62071424 and 62027805, in part by the Zhejiang Laboratory Foundation of China under Grant 2020KCDAB01, and in part by the Zhejiang Provincial Natural Science Foundation of China under Grant LD21F010002. The work of Hanzhi Ma was also supported by the Zhejiang University Academic Award for Outstanding Doctoral Candidates under Grant 202035. The work of Xu Chen was supported by the National Science Foundation under Grant CNS 16-24811 (Center for Advanced Electronics through Machine Learning). (Corresponding authors: Da Li; Er-Ping Li.)

Hanzhi Ma, Da Li, and Er-Ping Li are with the College of Information Science and Electronic Engineering, Zhejiang University–University of Illinois at Urbana–Champaign Institute, Zhejiang University, Hangzhou 310027, China (e-mail: mahanzhi@zju.edu.cn; li-da@zju.edu.cn; liep@zju.edu.cn).

Andreas C. Cangellaris and Xu Chen are with the Department of Electrical and Computer Engineering, University of Illinois at Urbana–Champaign, Urbana, IL 61820 USA (e-mail: cangella@illinois.edu; xuchen1@illinois.edu).

Digital Object Identifier 10.1109/TSIPI.2022.3173592

links is one of the most important and challenging problems in the design process as the operating frequency increases. On this basis, the optimization of high-dimensional design parameters is required to achieve a better high-speed system with higher quality signal transmission and minimal transmission errors.

In the high-speed link design procedure, designers always need to go through many iterations of trial and error to find a design that meets specifications. Different optimization methods, such as genetic algorithm [1] and Bayesian optimization, were employed with different iteration strategies for the inverse design of channel parameters [2], [3] and IBIS-AMI equalization settings [4], [5]. During iterations, traditional electronic design automation transient simulation tools (such as Keysight ADS, HSPICE, etc.) can achieve accurate performance assessment results but take a long simulation time that seriously affects and limits the design process of the system. Fast time-domain simulation technology is, then, developed to provide a faster simulation speed and higher efficiency; however, its linear timeinvariant assumption causes major limitations when analyzing the performance of the high-speed link with nonlinear characteristics. The multiple edge response method is, then, developed for nonlinear signal integrity analysis, but its nonlinear ability is closely related to order settings and has limitations for the links with heavier nonlinear behaviors [6]. Jitter budget enables nonlinear analysis as well; however, the independence between the subsystems' jitter is assumed in this approach [7]. On this basis, machine learning technology [8], [9] has attracted wide attention from researchers due to its powerful data learning and processing capabilities [10], [11]. Support vector machine [12], [13], neural networks [14], [15], and Gaussian process [16] have been widely explored in recent years as a surrogate model for efficient performance evaluation to speed up the iteration procedure in design optimization. The accuracy and efficiency of these surrogate models are compared with their application to the eye diagram prediction of different high-speed links [16], [17].

However, the machine-learning-driven inverse design still presents several technical challenges in the complex high-speed system with high-dimensional design parameters: 1) it is difficult to achieve relationship from the low-dimensional target space back to the high-dimensional design data; 2) a large amount of repeated simulation or measurement is needed to establish a surrogate model and verify that the optimal solution meets the constraint conditions; and 3) it is necessary to provide additional constraints into the algorithm to achieve a unique

2768-1866 © 2022 IEEE. Personal use is permitted, but republication/redistribution requires IEEE permission. See https://www.ieee.org/publications/rights/index.html for more information.

inverse problem solution. Utilizing dimensionality reduction techniques can help alleviate these challenges of the inverse design to a certain extent. Principal component analysis (PCA) [18] is utilized to map the high-dimensional tuning variables to a set of reduced dimension vectors and reduce the optimization iterations to achieve the design objective [19]. Nevertheless, the PCA method reduces dimensionality without considering the relationship between the input design parameters and outputs, which impacts high-speed link performance evaluation [20].

To address the aforementioned issues, a new optimization method that utilizes the support-vector-regression-based active subspace (SVR-AS) as the design space dimensionality reduction method is proposed in this article to accelerate the link optimization. The SVR-AS method [21], [22] identifies a set of directions along which the input perturbation mainly influences the output and generates a lower dimensional space named active variable, which presents its advantage of high-speed link performance assessment [20]. Aforementioned previous work proposed a forward modeling method from design parameters to outputs. This article mainly focuses on the inverse problem from target outputs to design parameters based on the dimensionality reduction ability of the SVR-AS forward modeling method. A simplified and mathematically solvable equation for the equality constrained design problem is proposed for the one-dimensional active variable [23]. This article builds on the foundation of [23], improves the inverse design ability by providing a generalized optimization algorithm for nonlinear equality and inequality constrained optimization problem that contains one- and multidimensional active variables generated from the SVR-AS method, and validates this algorithm using two different high-speed link design examples: channel parameter inverse design for the nonreturn-to-zero (NRZ) signal and IBIS-AMI equalization setting design for the four-level pulse amplitude modulation (PAM-4) signal. In our implementation, the active variable obtained by the linear weighted combination of the high-dimensional design space in the SVR-AS method is regarded as the lower dimensional optimization space. For each active variable, a simplified and mathematically solvable equation for finding optimal design parameter is derived in the proposed method. On this basis, active variable space helps accelerate the optimization procedure due to the lower space dimension, and we can efficiently obtain the final design variable from the optimal active variable. This developed method takes the advantage of reduced-dimensional space, utilizes simplified solvable equalization for the one-dimensional activate variable or optimize in multidimensional active variable space, and highly demonstrates its efficient optimal design for the nonlinear constrained optimization problem by examining for the analysis of two high-speed links against to the traditional interior-point method. Compared with [23], this article provides a more complete workflow to solve the inverse problem by adding: 1) the design optimization method for the multidimensional activate variable; 2) inequality constraint optimization method for both the one- and multidimensional activate variable; and 3) a practical example for IBIS-AMI PAM-4 equalization design. A generalized sensitivity analysis function based on the SVR-AS method is also presented for both the one- and multidimensional

active variable cases and verified by an equalization setting example.

The rest of this article is organized as follows. Section II details the proposed optimization methodology and sensitivity analysis function. Section III examines the proposed optimization algorithm for two high-speed link examples with channel design parameters under NRZ modulation and IBIS-AMI equalization settings under PAM-4 modulation, respectively. Finally, Section IV concludes this article.

II. METHODOLOGY

An optimization problem in an electronic system and a device design procedure is taken into account in this research, where it is to fine-tune the candidate design parameters generated from floor planning to satisfy the electrical performance specifications. In other words, an optimal design closest to a prototype design is necessary to obtain where the output requirements are satisfied. In addition, speed is essential for the optimization method to support fast "what if" analysis; thus, different design scenarios are quickly compared to see which one is feasible.

Let $X = [x_1, \dots, x_p]^{\mathrm{T}}$ be the input p-dimensional normalized design parameter space, x_i is normalized to range [-1,1], Y represents the output of interest, $D = \{(\boldsymbol{X_1}, Y_1), \dots (\boldsymbol{X_n}, Y_n)\}$ represents the sampling dataset, and function h is the nonlinear mapping from \boldsymbol{X} to Y. As illustrated, the optimization objective is to find a set of \boldsymbol{X} that is closet to a set of candidate design $\boldsymbol{X_0}$ (where $x_i = 0$) for desired output Y_0 or desired output range $[Y_{\min}, Y_{\max}]$. The mean squared distance (MSD) between \boldsymbol{X} and the nominal numbers is used as the fine-tuning cost; thus, the optimization problem can be expressed as

$$\min g\left(\boldsymbol{X}\right) = \frac{1}{p} \sum_{1 \le i \le p} x_i^2$$
 s.t. $h\left(\boldsymbol{X}\right) = Y_0$ (1)

or

$$\min g(\boldsymbol{X}) = \frac{1}{p} \sum_{1 \le i \le p} x_i^2$$

$$\text{s.t.} h(\boldsymbol{X}) \in [Y_{\min}, Y_{\max}]. \tag{2}$$

A. Optimization Solution in Active Subspace

The optimization algorithm with dimensionality reduction takes advantage of lower dimensional input space to help obtain the optimal solution with the extension of the SVR-AS method, where SVR-AS [21] is used for sensitivity analysis and dimensionality reduction by utilizing the differential expression of a support vector regression (SVR) prediction function, and to identify a set of important directions in the space of all input parameters.

The SVR-AS method utilizes a symmetric and positivelysemidefinite matrix Z with the SVR prediction function

$$Z = \frac{1}{n} \sum_{1 \le i \le n} \nabla_{X} F(X_i) \left(\nabla_{X} F(X_i) \right)^{\mathrm{T}}$$
(3)

$$F(\mathbf{X}) = \sum_{1 \le i \le n} (\alpha_i' - \alpha_i) \exp\left(-\frac{1}{2\sigma^2} \|\mathbf{X} - \mathbf{X}_i\|^2\right) + b$$
(4)

where $\alpha_i \geq 0$ and $\alpha_i' \geq 0$ are Lagrange multipliers, b is the displacement of hyperplane, and $\sigma > 0$ is the width of Gaussian kernel.

The active variable, a lower dimensional representation of the input parameters, is defined as

$$\boldsymbol{v} = \boldsymbol{W}_{1}^{\mathrm{T}} \boldsymbol{X} \tag{5}$$

where active subspace W_1 represents the partial set of eigenvectors in eigendecomposition $Z = W\Lambda W^T$, corresponding to the largest q eigenvalues Λ_1 , and its perturbation in the input has the largest impact on the output [24].

The new optimization algorithm is extended based on the SVR-AS method since it provides a lower dimensional active variable space as a linear weighted combination of the input design parameters. In such reduced-dimensional space, for each active variable v_0 , there is a unique set of input design parameters with minimum MSD from candidate design X_0 (normalized to $x_i=0$). The optimization problem for each active variable v_0 is expressed as

$$\min g(\mathbf{X}) = \frac{1}{p} \sum_{1 \le i \le p} x_i^2$$

$$\text{s.t.} \phi(\mathbf{X}) = \mathbf{W}_1^{\text{T}} \mathbf{X} - \mathbf{v}_0 = 0.$$
 (6)

This linear constrained optimal problem can be solved by the Lagrange multiplier method. The Lagrange function for (6) is described as

$$L(X, \lambda) = q(X) + \beta \phi(X) \tag{7}$$

where $\beta = [\beta_1, ..., \beta_q]$ are the Lagrangian multipliers. Thus, the optimal design parameters can be expressed as

$$\boldsymbol{X}_{\text{opt}} = \boldsymbol{W}_1 \left(\boldsymbol{W}_1^{\text{T}} \boldsymbol{W}_1 \right)^{-1} \boldsymbol{v}_0. \tag{8}$$

In practice, it is common that several design parameters are fixed at specific values due to design requirements and, thus, not in the set of optimization variables. For these requirements, suppose that Ω represents the indices of specific design parameters, and

$$\boldsymbol{X}_{\text{fix}} = \begin{cases} x_{i_j}, & \text{if } i_j \in \Omega \\ 0, & \text{others} \end{cases}$$
 (9)

$$\boldsymbol{X}_{\text{unfix}} = \begin{cases} 0, & \text{if } i_j \in \Omega \\ x_{i_j}, & \text{others} \end{cases}$$
 (10)

 $m{W}_1$ can also be divided into $m{W}_{ ext{fix}}$ and $m{W}_{ ext{unfix}}$ similarly. Thus

$$v = W_{\text{fix}}^{\text{T}} X_{\text{fix}} + W_{\text{unfix}}^{\text{T}} X_{\text{unfix}}$$
 (11)

and a variant of (8) is expressed as

$$oldsymbol{X}_{ ext{opt}} = oldsymbol{W}_{ ext{unfix}} \left(oldsymbol{W}_{ ext{unfix}}^{ ext{T}} oldsymbol{W}_{ ext{unfix}}
ight)^{-1} \left(oldsymbol{v}_0 - oldsymbol{W}_{ ext{fix}}^{ ext{T}} oldsymbol{X}_{ ext{fix}}
ight) + oldsymbol{X}_{ ext{fix}}.$$

In this way, (8) and (12) directly provide the optimal design with minimum MSD for each active variable with extremely

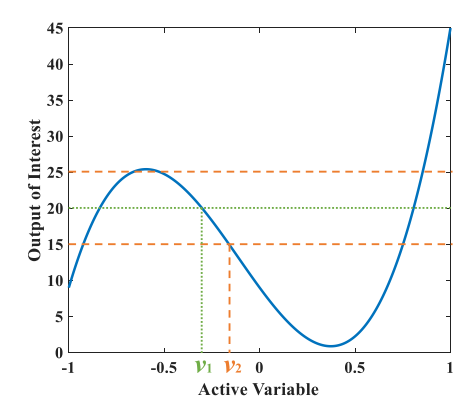


Fig. 1. Sufficient summary plot from active variable to output of interest.

low computation burden as it will be demonstrated later in this article.

B. Optimization Algorithm for One-Dimensional Active Subspace

For the case where the active space generated by the SVR-AS method is one-dimensional, the relationship between the active variable and the output of interest can be plotted as a one-to-one or many-to-one mapping in a 2-D figure, which can be fitted using a polynomial function:

$$Y = P(v) = c_n v^n + \dots + c_1 v + c_0 \tag{13}$$

where c_0,\ldots,c_n are the coefficients of polynomial approximation. It is clear that the closer the active variable is to zero, the smaller the MSD of the optimal design parameters due to (8) and (12). Fig. 1 depicts a sufficient summary plot example between the one-dimensional active variable and the output of interest, where v_1 is the active variable with the smallest MSD of the design parameter when the output equal to 20 is required and v_2 is the selected active variable when the output should be in range from 15 to 25.

In this way, the original optimization design problem (1) can be separated as two optimization steps: find minimum $abs(v_0)$ for desired output Y_0 or desired output range $[Y_{\min}, Y_{\max}]$ by the root function of the polynomial equation and then find the optimal design X_{opt} for v_0 . The first step can be expressed as

min abs
$$(v_0)$$

s.t. $P(v_0) = Y_0$ (14)

or

min abs
$$(v_0)$$

s.t. $P(v_0) \in [Y_{\min}, Y_{\max}].$ (15)

With this in mind, Algorithm 1 depicts the optimization algorithm for one-dimensional active subspace.

As shown in Algorithm 1, the SVR-AS method is first used to calculate the active variable from the training dataset, followed by fitting the relationship between the active variable and the output of interest using the polynomial function; then, the minimum absolute active variable for the desired output is identified, and the optimal result can be finally calculated.

Algorithm 1: Optimization Algorithm for One-Dimensional Active Subspace.

Input: Desired output Y_0 or output range $[Y_{\min}, Y_{\max}]$, Training dataset $D = \{(\boldsymbol{X_1}, Y_1), \dots (\boldsymbol{X_n}, Y_n)\}$.

Output: Optimal design X_{optimal} .

- 1: Calculate active variables v for D by SVR-AS method via (5).
- 2: Approximate the relationship between v and Y via (13).
- 3: Solve (13) with $P(v) = Y_0$ or $P(v) = Y_{\min}$ and $P(v) = Y_{\max}$.
- 4: Determine the minimum absolute v_0 as (14) or (15).
- 5: Calculate the optimal design X_{optimal} via (8) or (12).

C. Optimization Algorithm for Multidimensional Active Subspace

Calculating the optimal design for r-dimensional active variable (1 < r < p) example is much more difficult since the relationship between the active variable and the output of interest is more complex.

For the optimization problem with multidimensional active subspace, the SVR-AS-based optimization problem uses a new SVR model to fit the relationship between active variables and output with a training dataset $E = \{(v_1, Y_1), \ldots (v_m, Y_m)\}$ sampled from the space of active variables. Previous work [20] shows that the SVR model with the active variable as input has the advantage of better accuracy and less training dataset.

The new trained SVR model in active variable space can be expressed as

$$G(\boldsymbol{v}) = \sum_{1 \le i \le m} (\alpha_i' - \alpha_i) \exp\left(-\frac{1}{2\sigma^2} \|\boldsymbol{v} - \boldsymbol{v}_i\|^2\right) + b.$$
 (16)

Then, the optimization problem changes to

min MSE
$$\left(\boldsymbol{W}_{1} \left(\boldsymbol{W}_{1}^{\mathrm{T}} \boldsymbol{W}_{1} \right)^{-1} \boldsymbol{v}_{0} \right)$$

s.t. $G\left(\boldsymbol{v}_{0} \right) = Y_{0}$ (17)

or

min MSE
$$\left(\boldsymbol{W}_{1}\left(\boldsymbol{W}_{1}^{\mathrm{T}}\boldsymbol{W}_{1}\right)^{-1}\boldsymbol{v}_{0}\right)$$

s.t. $G\left(\boldsymbol{v}_{0}\right) \in [Y_{\mathrm{min}}, Y_{\mathrm{max}}].$ (18)

Thus, in this way, we optimize in the low-dimensional active variable space rather than the original design space with lower cost of computation burden using the traditional optimization method, e.g., interior point method.

Algorithm 2 shows the optimization method for multidimensional active subspace. The SVR-AS method is first used to calculate the active variables from the training dataset. Then, we generate a new smaller dataset in active variable subspace and find a new SVR predictive function between active variables and the corresponding output. In this way, we use the optimization method, e.g., interior point method, to calculate the optimal active variables for the desired output and then calculate the optimal result. Note that the result from such an optimization problem is not unique.

Algorithm 2: Optimization Algorithm for Multidimensional Active Subspace.

Input: Desired output Y_0 or output range $[Y_{\min}, Y_{\max}]$, Training dataset $D = \{(X_1, Y_1), \dots (X_n, Y_n)\}$.

Output: Optimal design $oldsymbol{X}_{ ext{optimal}}$

- 1. Calculate active variables v for D by the SVR-AS method via (5).
- 2. Generate dataset $E = \{(v_1, Y_1), ..., (v_m, Y_m)\}$ in active variable subspace.
- 3. Calculate the new SVR prediction model for E via (16).
- 4. Find optimal v_0 via (17) or (18).
- 5. Calculate the optimal design X_{optimal} by (8) or (12).

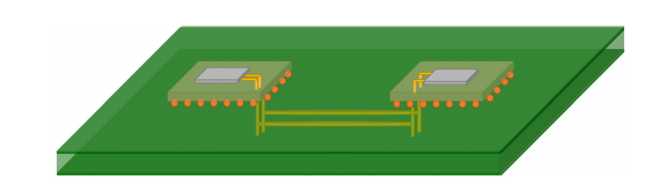


Fig. 2. High-speed chip-to-chip serial link.

Previous work [21] illustrates sensitivity analysis from the SVR-AS method for the one-dimensional active subspace example, whose results fitted well with the Sobol total index. This article further illustrates sensitivity analysis realized by the SVR-AS algorithm for the multidimensional active subspace.

In the SVR-AS algorithm, eigenvectors represent the important directions along which perturbation in the input has the impact on the output; thus, eigendecomposition of \boldsymbol{Z} provides an intuitive way for the sensitivity analysis of input parameters. Activity scores can be used as a comprehensive and justifiable sensitivity metric

$$a_k = a_k(q) = \frac{\sum_{1 \le r \le q} \lambda_r w_{k,r}^2}{\sum_{1 \le r \le q} \lambda_r}.$$
 (19)

These numbers rank the importance of a model's inputs using the largest eigenvalue Λ_1 with its corresponding eigenvector W_1 . For the one-dimensional active variable, the activity scores can be simplified as

$$a_k = a_k(q) = w_{k,1}^2 (20)$$

which is consistent with the usage of absolute eigenvector values in previous work [21].

III. APPLICATION TO HIGH-SPEED LINK INVERSE DESIGN

A. Example I: Channel Design Variables Under NRZ Modulation

The first example chosen to evaluate the proposed method is the optimization of a channel with 16 design parameters in a high-speed chip-to-chip serial link, as shown in Fig. 2. In this link, the NRZ signal passes through a transmitter (Tx), differential microstrip line, land grid array (LGA) model, via model, differential strip line, via model, LGA, microstrip line, and receiver (Rx). The output of interest is the eye opening characteristic of

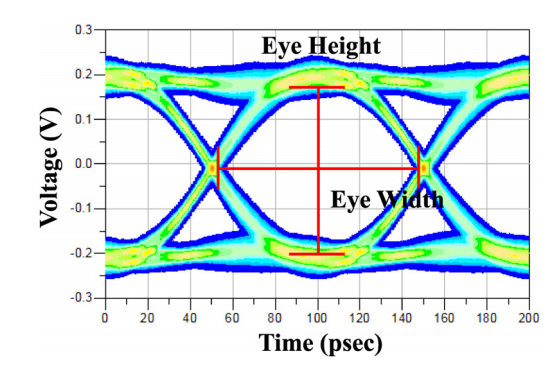


Fig. 3. Eye diagram of a high-speed link for the NRZ signal.

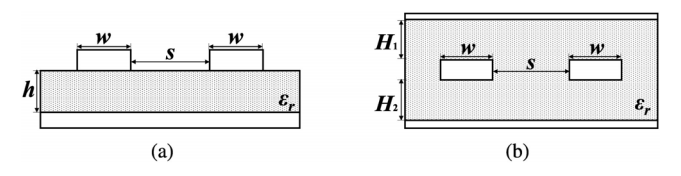


Fig. 4. Cross-sectional geometries of the microstrip line and the strip line. (a) Microstrip line. (b) Strip line.

TABLE I
DESIGN PARAMETERS OF EXAMPLE I

	Parameter	Nominal value	Range
	ε_r	4.4	3.6-5.2
Tx Microstrip	w	5 mil	4.5-5.5 mil
Line	s	8 mil	7.2-8.8 mil
Line	h	4 mil	3.7-4.3 mil
	l	11 mm	2-20 mm
	ε_r	4.4	3.6-5.2
	w	5 mil	4.5-5.5 mil
Strip Line	s	8 mil	7.2-8.8 mil
Suip Line	H_1	8 mil	7.2-8.8 mil
	H_2	8 mil	7.2-8.8 mil
	l	275 mm	50-500 mm
Rx Microstrip	ε_r	4.4	3.6-5.2
	w	5 mil	4.5-5.5 mil
Line	s	8 mil	7.2-8.8 mil
Line	h	4 mil	3.7-4.3 mil
	l	11 mm	2-20 mm

the channel, as depicted in Fig. 3, which is obtained through a statistical high-speed link analysisin Keysight ADS [25] using commercial IBIS-AMI behavioral I/O models for Tx and Rx, including effects from a Tx finite-impulse response (FIR) filter, an Rx continuous-time linear equalizer (CTLE), and an Rx decision feedback equalizer (DFE). Eye width, the distance between the three-sigma points of the crossing time histograms, is treated as a representative output parameter in this article.

For this example, the design parameters are associated with the cross-sectional geometries of the Tx microstrip line, the strip line, and the Rx microstrip line, as shown in Fig. 4(a) and (b). Table I summarizes the nominal value and the optimization range of the 16 geometric design parameters associated with the lines. These 16 parameters constitute an input parameter space of relatively high dimensionality such that a brute-force parameter sweep for design optimization is intractable.

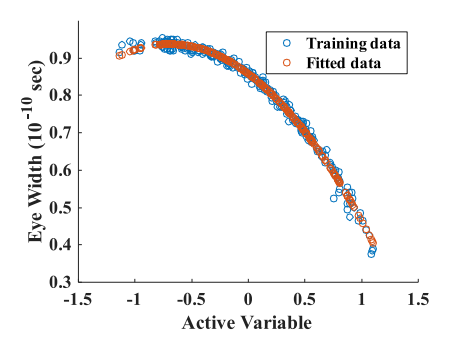


Fig. 5. Sufficient summary plot of Example I and its fitted function.

The SVR-AS-based optimization method helps to find the optimal 16 design parameters for the desired output. The first step of Algorithm 1 is to generate a reduced-dimension active variable space from the original 16 design parameter space. R^2 score is treated as a statistical measure for the SVR regression model, which is always in the range from 0 to 1. The closer the R^2 -score gets to 1, the better the model predicts. In this article, a well-trained SVR model with 0.9996 and 0.9832 R^2 -score for 250 training samples and 3000 test samples is utilized to generated active variable, a one-dimensional linear combination of 16 design parameters, since the first eigenvalue is much larger than the others. Fig. 5 shows the sufficient summary plot between the active variable and the corresponding eye width. As the second step in Algorithm 1, a second-order polynomial function $(Y = -0.1644v^2 - 0.2294v + 0.8579)$ shown in orange color approximates this relationship well with 0.9923 R^2 -score.

Table II illustrates the optimization results for the desired eye width output from the SVR-AS-based optimization method. Equation (14) is used to calculate the active variable when the desired eye width is a specific value $(7.5 \times 10^{-11} \text{ s in})$ Table II), while (15) is applied when the eye width range is required for optimization. In real fabrication, we can only use the ε_r value provided by the processing manufacturer to design channel and cannot preset its manufacturing error. Since the SVR-AS forward model is generated from variables in Table I $(\varepsilon_r \text{ included}), \varepsilon_r \text{ can be set as different values for the channel}$ inverse design within the range in Table I to fit with different manufacturer's data. In this example, we fix dielectric constant as $\varepsilon_r = 4.4$ due to the requirement of practical design, and the optimal design parameter is calculated by (12) from the active variable. Traditionally, the interior-point method can solve nonlinear constrained minimization problem through a sequence of approximation problems. Table II also shows the optimization results calculated by this traditional optimization method as a comparison of the SVR-AS-based method. Eye width is evaluated by the SVR predictive model in its iterative process. Jointly calling ANSYS Q3D Extractor [26] and Keysight ADS can also be used in the optimization stage to replace the surrogate model with larger computational burden.

Results from Table II show that both the SVR-AS-based optimization method and the traditional interior-point method can find an optimal design for the required eye width output with fine-tuning purpose. Compared with the traditional method,

Objective	SVR-A	SVR-AS based Optimization Method		Traditional Optimization Method		
Eye Width (10 ⁻¹⁰ sec)	Time (sec)	Eye Width of Optimal Design (10^{-10} sec)	Normalized MSD of Optimal Design	Time (sec)	Eye Width of Optimal Design (10^{-10} sec)	Normalized MSD of Optimal Design
= 0.75	7.67×10^{-4}	0.750	0.0089	14.72	0.745	0.0089
≥ 0.8	0	0.855	0	0.27	0.855	0
≤ 0.7	8.03×10^{-4}	0.700	0.0164	8.76	0.700	0.0164
[0.6, 0.8]	7.66×10^{-4}	0.800	0.0031	25.32	0.800	0.0032
[0.7, 0.9]	0	0.855	0	0.26	0.855	0

TABLE II EXAMPLE I RESULTS

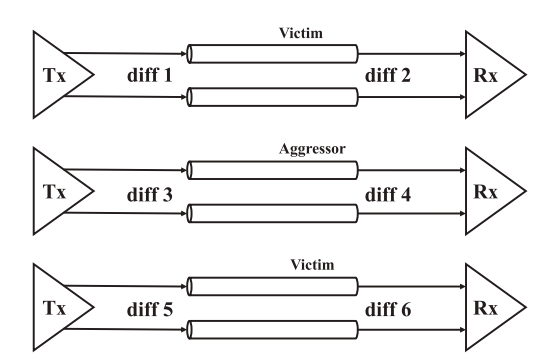


Fig. 6. High-speed link with crosstalk for PAM-4 signal modulation.

which calls the SVR surrogate model repeatedly during the iterations process, the proposed SVR-AS-based optimization method works well with four orders of magnitude reduction in computation cost for both the equality and inequality constraints. The design objective in this article is to obtain an optimal design closest to a prototype design where the eye opening requirements are satisfied. Basis on this, differential trace impedance will change as little as possible since we expect to make the smallest change of the initial design. In this example, the differential impedance of the nominal Rx microstrip line design is $100.5~\Omega$, and the optimal results in Table II all have $100.5-\Omega$ differential impedance. In addition, it is worth to mention that the SVR-AS-based optimization method can quickly calculate lots of different settings that satisfy different specific requirements (e.g., we can also keep $\varepsilon_r = 4.2$ or w = 5 mil).

B. Example II: PAM-4 IBIS-AMI Equalization Settings

This example concerns the optimization of IBIS-AMI equalization setting in a high-speed link with crosstalk for PAM-4 signal modulation at 10-Gb/s rate, as shown in Fig. 6. The physical channel consists of a microstrip line, connected through an LGA and a via to a strip line, which in turn is connected to a microstrip line through a via and an LGA. The cross-sectional geometry details of the differential microstrip line and the differential strip line are shown in Fig. 7. Fig. 8 depicts the differential S parameters of the whole channel obtained from Keysight ADS.

Fig. 9 illustrates the IBIS-AMI equalizer used in the Tx and the Rx. The PAM-4 Tx model is an equalizer implemented with an FIR filter, where the first three filter taps, Tap(0), Tap(1), and Tap(2), are considered in this example. The PAM-4 Rx model includes a CTLE, a feedforward equalizer (FFE), a clock data recovery (CDR) unit, and a DFE. The input signal flows to

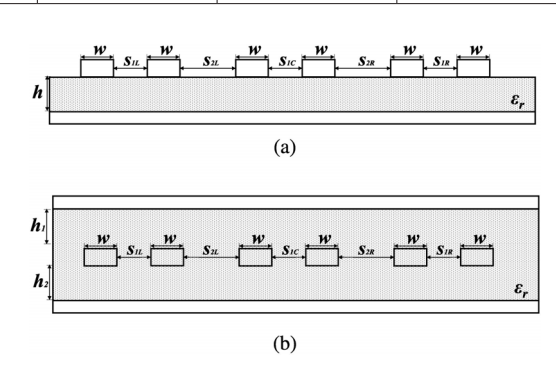


Fig. 7. Cross-sectional geometries of lines. (a) 10-mm microstrip line. (b) 200-mm strip line (w=8mil; $H=H_1=H_2=6$ mil; $S_{1L}=S_{1C}=S_{1R}=12$ mil; $S_{2L}=S_{2R}=16$ mil; $\varepsilon_r=4.4$).

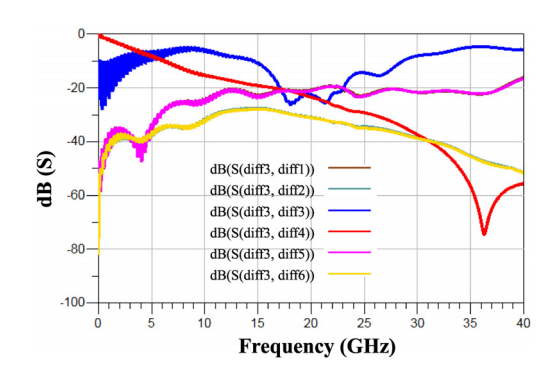


Fig. 8. S-parameter for the channel in Example II.

CTLE, FFE, and DFE to output in sequence. The FFE output is also fed to CDR, which recovers the clock signal for DFE to determine the optimized decision point. The CTLE transfer function in the *s*-domain can be expressed as

$$H(s) = f \frac{(s - z(0)) \cdots (s - z(N_z - 1))}{(s - p(0)) \cdots (s - p(N_p - 1))}$$
(21)

where f is the CTLE factor, z(i) is the ith CTLE zero, p(i) is the ith CTLE pole, N_z is the number of zeros, and N_p is the number of poles. The DFE is used to cancel residual postcursor intersymbol interference, whose output is determined by the input and previous decision results. The least mean square adaptation algorithm is used to update the filter taps automatically with the adaptation coefficient α

$$Tap_{DFE}[i](n) = Tap_{DFE}[i](n-1) - \alpha * \xi * d(n-1) \quad (22)$$

where $\text{Tap}_{\text{DFE}}[i](n)$ is the current value of the *i*th DFE Tap, $\text{Tap}_{\text{DFE}}[i](n-1)$ is its previous value, ξ is the error between

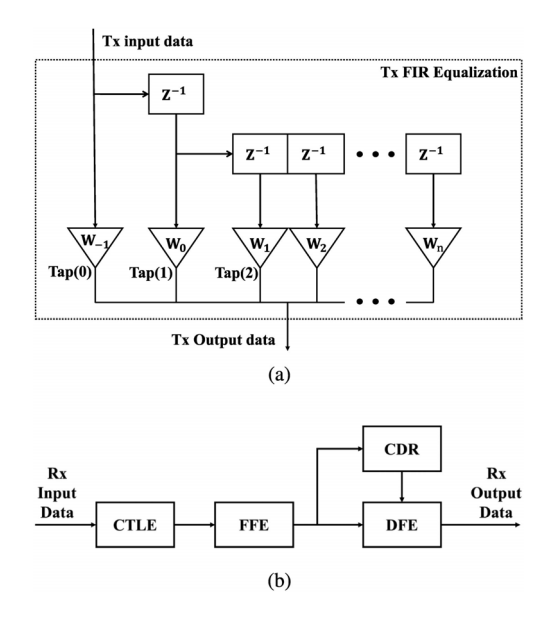


Fig. 9. Tx and Rx equalization model.

TABLE III
IBIS-AMI EQUALIZATION SETTINGS OF EXAMPLE II

	Parameter	Nominal value	Range
	Tap(0)	0	[-0.1, 0.1]
Tx FIR	Tap(0)		
IX FIK	Tap(1) 0.8		[0.7, 0.9]
	Tap(2)	-0.2	-{1- Tap
	F(-)	V. <u>-</u>	[0]l-lTap [1]l}
			$[2.5 \times 10^{11},$
	f	$3 \times 10^{11} \text{ Hz}$	3.5×10^{11}]
Rx CTLE			Hz
KX CILL	p(0)	$-5 \times 10^{9} \text{ Hz}$	$[-6 \times 10^9,$
	p(0)	-5 × 10 HZ	-4×10^{9}] Hz
	p(1)	$-10 \times 10^{9} \text{ Hz}$	$[-11 \times 10^9,$
		-10 × 10 11Z	-9×10^{9}] Hz
	z(0)	$-3 \times 10^{9} \text{ Hz}$	$[-4 \times 10^9,$
		-3 × 10 11Z	-2×10^{9}] Hz
Rx DFE	α	0.005	[0.0005, 0.002]

decision and output sample, and d(n-1) is the decision output of the previous output sample.

This work focuses on seven independent and one dependent equalization settings on Tx FIR, Rx CTLE, and Rx DFE.Rx CDR and Rx FFE are fixed in this example. The nominal values and ranges of the equalization variables are recorded in Table III. Fig. 10 depicts the eye opening after Rx calculated from Keysight ADS with nominal equalization settings. The output of interest is the minimum eye height in the PAM-4 eye diagram

$$H_{PAM-4} = min(H_{top}, H_{middle}, H_{bottom}).$$
 (23)

For this example, the SVR-AS method is helpful in reducing the original design space into a 2-D active variable space after using 250 training data samples to establish the SVR model between equalization settings and eye height $H_{\rm PAM-4}$. A sufficient summary plot in Fig. 11 depicts that the relationship between equalization settings and eye height is more clearly identified by the 2-D active viable vector. In this way, owing to the multidimensional active subspace, a second SVR model is

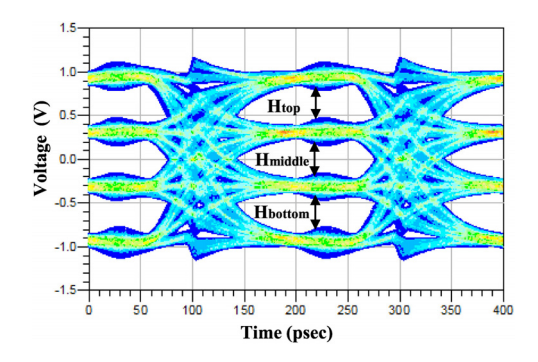


Fig. 10. PAM-4 eye diagram of Example II.

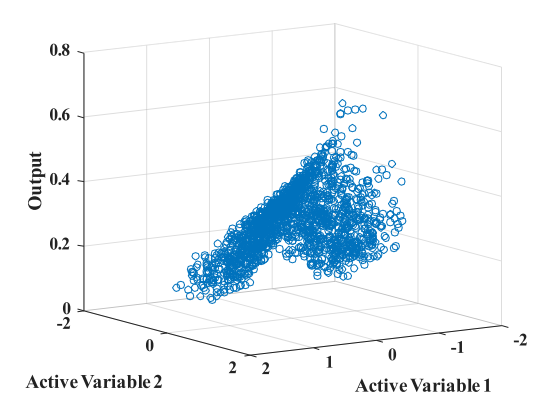


Fig. 11. Sufficient summary plot of Example II.

TABLE IV SVR Model Established in Example II

	SVR-AS based C	Traditional Optimiza- tion Method	
	SVR Model in Design Space SVR Model in Active Variable Space		SVR Model in Design Space
Training Set	250	50	300
Testing Set	1500 1500		1500
Training R^2 -Score	0.9801	0.9993	0.9746
Testing R^2 -Score	0.9495	0.9672	0.9499
Training MSE (V ²)	2.46×10^{-4}	1.52×10^{-5}	3.08×10^{-4}
Testing MSE (V ²)	6.15×10^{-4}	3.99×10^{-4}	6.09×10^{-4}

established in the active variable space with 50 new active variables samples for design optimization. In this way, the SVR-AS-based optimization method will find the optimal active variables first based on the SVR model in the active variable space and then calculate optimal equalization settings, as illustrated in Algorithm 2. For fair comparison, as shown in Table IV, the traditional optimization method uses the same amount of training samples (250+50=300) and directly optimizes the design parameter by the SVR model established with 300 training samples in the original design space. Prediction results in Table IV show that the SVR model established in the active variable space has a better

Objective	SVR-A	SVR-AS based Optimization Method		Traditional Optimization Method		
H _{PAM-4} (V)	Time (sec)	H _{PAM-4} of Optimal Design (V)	Normalized MSD of Optimal Design	Time (sec)	H _{PAM-4} of Optimal Design (V)	Normalized MSD of Optimal Design
= 0.25	1.86	0.251	0.0525	10.84	0.240	0.0564
≥ 0.35	0.08	0.412	0	0.17	0.412	0
≤ 0.15	2.16	0.150	0.1319	12.08	0.158	0.1066
[0.1, 0.3]	2.13	0.292	0.0262	12.49	0.292	0.0314
[0.3, 0.5]	0.08	0.412	0	0.17	0.412	0

TABLE V EXAMPLE II RESULTS

TABLE VI SENSITIVITY ANALYSIS RESULTS BY THE SVR-AS METHOD AND THE SOBOL METHOD

Parameter	SVR-AS	Method	Sobol Method		
1 arameter	a_k	Rank	ST	Rank	
Tap(0)	0.8427	1	0.5274	1	
Tap(1)	0.0726	2	0.2211	2	
f	0.0218	5	0.0772	4	
p(0)	0.0276	3	0.0630	5	
p(1)	0.0117	6	0.0219	6	
z(0)	0.0221	4	0.0841	3	
α	0.0015	7	0.0042	7	

prediction performance of R^2 -score and mean squared error (MSE) due to the direction in which the input disturbance that affects the output most is found during dimensionality reduction.

Table V describes the optimization results for the desired eye height output or output range generated from the proposed method and the traditional method, respectively. Both the SVR-AS-based optimization method and the traditional interior-point method can provide an optimal result for equality and inequality constraints. The proposed SVR-AS-based optimization method gets a more accurate result due to the better prediction performance of SVR in the active variable space and has the advantage of optimization time since it optimizes in a lower dimensional space.

Table VI illustrates the sensitivity analysis results for seven independent parameters in this example based on the SVR-AS method compared with the traditional Sobol method [27]. Activity scores calculated by (19) and total Sobol indices ST both illustrate that in this example, Tap(0) and Tap(1) are the top-2 important parameters, while p(1) and α are the least important parameters. The SVR-AS method provides an accurate sensitivity ranking of design parameters when it only needs 250 training samples to establish the SVR model rather than using more than 1200 data samples to calculate total Sobol indices.

IV. CONCLUSION

In this article, a fast constrained optimization method based on SVR-AS is developed for a high-speed link design process, which takes advantage of active subspace, a reduced-dimensional space calculated from a linear weighted combination of a higher dimensional design space. In particular, this method is able to transform the complex nonlinear constrained optimization into a linear constrained minimization problem for both equality and inequality constraints. A directly solvable function is provided by the proposed method to calculate

the optimal results associated with each active variable. Two optimization algorithms are illustrated in this article for the design optimization problem: one for the case of one-dimensional active variable subspace and one for the case of multidimensional activate subspace. Two high-speed link design examples, one with channel parameters for NRZ pulse and the other with equalization settings for the PAM-4 signal, are used to demonstrate the use of the proposed algorithms. Compared with the traditional interior-point method, the proposed method is able to efficiently and accurately find the optimal design settings more efficiently and accurately. The sensitivity analysis ability of the SVR-AS method is also elaborated for the multidimensional active variable example. The proposed SVR-AS optimization method can be utilized to more complex high-speed link examples including interconnection parameters in the future work. Considering channel operating margin is a fast and efficient mean to assign a single figure of merit to interconnect channels, comparing our method with channel operating margin is an ongoing research topic. This optimization method also has a great potential to be applied in other microwave circuits and components designs, and its corresponding discrete variable optimization algorithm is still need to be explored.

REFERENCES

- [1] H. Kim, C. Sui, K. Cai, B. Sen, and J. Fan, "Fast and precise high-speed channel modeling and optimization technique based on machine learning," *IEEE Trans. Electromagn. Compat.*, vol. 60, no. 6, pp. 2049–2052, Dec. 2018.
- [2] H. M. Torun and M. Swaminathan, "High-dimensional global optimization method for high-frequency electronic design," *IEEE Trans. Microw. Theory Techn.*, vol. 67, no. 6, pp. 2128–2142, Jun. 2019.
- [3] D. Lho *et al.*, "Bayesian optimization of high-speed channel for signal integrity analysis," in *Proc. IEEE 28th Conf. Elect. Perform. Electron. Packag. Syst.*, Montreal, QC, Canada, Oct. 2019, pp. 1–3.
- [4] Z. Kiguradze et al., "High-speed channel equalization applying parallel Bayesian machine learning," in Proc. IEEE Int. Symp. Electromagn. Compat. Signal/Power Integrity, Reno, NV, USA, 2020, pp. 251–256.
- [5] X. Yang et al., "Parallel Bayesian active learning using dropout for optimizing high-speed channel equalization," in Proc. IEEE 30th Conf. Elect. Perform. Electron. Packag. Syst., Oct. 2021, pp. 1–3.
- [6] X. Chu, W. Wang, J. Wang, Y. Li, and H. Wu, "Modeling and analysis of nonlinear high-speed links," in *Proc. IEEE Int. Symp. Electromagn. Compat. Signal/Power Integrity*, New Orleans, LA, USA, Jul. 2019, pp. 475–480.
- [7] M. P. Li, Jitter, Noise, and Signal Integrity at High-Speed. Upper Saddle River, NJ, USA: Prentice-Hall, 2008.
- [8] R. Trinchero, P. Manfredi, I. S. Stievano, and F. G. Canavero, "Machine learning for the performance assessment of high-speed links," *IEEE Trans. Electromagn. Compat.*, vol. 60, no. 6, pp. 1627–1634, Dec. 2018.
- [9] D. Lho et al., "Channel characteristic-based deep neural network models for accurate eye diagram estimation in high bandwidth memory (HBM) silicon interposer," *IEEE Trans. Electromagn. Compat.*, vol. 64, no. 1, pp. 196–208, Feb. 2022.

- [10] M. A. Dolatsara, J. A. Hejase, W. D. Becker, J. Kim, S. K. Lim, and M. Swaminathan, "Worst-case eye analysis of high-speed channels based on Bayesian optimization," *IEEE Trans. Electromagn. Compat.*, vol. 63, no. 1, pp. 246–258, Feb. 2021.
- [11] J. Reddy *et al.*, "Fast and accurate modeling of PCB differential trace skew compensation using ML," in *Proc. IEEE 30th Conf. Elect. Perform. Electron. Packag. Syst.*, Oct. 2021, pp. 1–3.
- [12] T. Lu, J. Sun, K. Wu, and Z. Yang, "High-speed channel modeling with machine learning methods for signal integrity analysis," *IEEE Trans. Electromagn. Compat.*, vol. 60, no. 6, pp. 1957–1964, Dec. 2018.
- [13] R. Trinchero and F. G. Canavero, "Modeling of eye diagram height in high-speed links via support vector machine," in *Proc. IEEE 22nd Workshop Signal Power Integrity*, Brest, France, May 2018, pp. 1–4.
- [14] X. Wang, T. Nguyen, and J. E. Schutt-Aine, "Laguerrevolterra feed-forward neural network for modeling PAM-4 high-speed links," *IEEE Trans. Compon., Packag., Manuf. Technol.*, vol. 10, no. 12, pp. 2061–2071, Dec. 2020.
- [15] M. A. Dolatsara, H. Yu, J. A. Hejase, W. D. Becker, and M. Swaminathan, "Invertible neural networks for inverse design of CTLE in high-speed channels," in *Proc. IEEE Elect. Des. Adv. Packag. Syst.*, Shenzhen, China, Dec. 2020, pp. 1–3.
- [16] T. Nguyen et al., "Comparative study of surrogate modeling methods for signal integrity and microwave circuit applications," *IEEE Trans. Com*pon., Packag., Manuf. Technol., vol. 11, no. 9, pp. 1369–1379, Sep. 2021.
- [17] H. Ma, E.-P. Li, A. C. Cangellaris, and X. Chen, "Comparison of machine learning techniques for predictive modeling of high-speed links," in *Proc. IEEE 28th Conf. Elect. Perform. Electron. Packag. Syst.*, Montreal, QC, Canada, Oct. 2019, pp. 1–3.
- [18] J. S. Ochoa and A. C. Cangellaris, "Random-space dimensionality reduction for expedient yield estimation of passive microwave structures," *IEEE Trans. Microw. Theory Techn.*, vol. 61, no. 12, pp. 4313–4321, Dec. 2013.
- [19] T. Zhu, C. Yongjin, C. Jacky, and C. Chris, "Accelerating 56G PAM4 link equalization optimization using machine learning-based analysis," in *Proc. Semicond. Electron. Des. Conf.*, 2019.
- [20] H. Ma, E.-P. Li, A. C. Cangellaris, and X. Chen, "Expedient prediction of eye opening of high-speed links with input design space dimensionality reduction," in *Proc. IEEE Int. Symp. Electromagn. Compat. Signal/Power Integrity*, Reno, NV, USA, 2020, pp. 236–240.
- [21] H. Ma, E.-P. Li, A. C. Cangellaris, and X. Chen, "Support vector regression-based active subspace (SVR-AS) modeling of high-speed links for fast and accurate sensitivity analysis," *IEEE Access*, vol. 8, pp. 74339– 74348, 2020.
- [22] H. Ma, "Sensitivity analysis of high-speed links with design space dimensionality reduction," in Proc. IEEE MTT-S Int. Conf. Electromagn. Multiphys. Model. Optim., 2020.
- [23] H. Ma, E.-P. Li, A. C. Cangellaris, and X. Chen, "High-speed link design optimization using machine learning SVR-AS method," in *Proc. IEEE* 29th Conf. Elect. Perform. Electron. Packag. Syst. (EPEPS). San Jose, CA, USA, Oct. 2020, pp. 1–3.
- [24] P. G. Constantine, B. Zaharatos, and M. Campanelli, "Discovering an active subspace in a single-diode solar cell model: Active subspaces in solar cells," *Statist. Anal. Data Mining*: ASA Data Sci. J., vol. 8, nos. 5/6, pp. 264–273, Oct. 2015.
- [25] Advanced Design System, Release 2019, Keysight, Santa Rosa, CA, USA, 2019.
- [26] ANSYS® Q3D Extractor Release 18.0, Ansys, Canonsburg, PA, USA.
- [27] J. Nossent, P. Elsen, and W. Bauwens, "Sobol' sensitivity analysis of a complex environmental model," *Environ. Model. Software*, vol. 26, no. 12, pp. 1515–1525, Dec. 2011.



Hanzhi Ma (Graduate Student Member, IEEE) received the B.S. degree in engineering, in 2017, from Zhejiang University, Hangzhou, China, where she is currently working toward the Ph.D. degree with the College of Information Science and Electronic Engineering, Zhejiang University–University of Illinois at Urbana–Champaign Institute.

Her current research interests include machine learning techniques for electromagnetic interference/severity index/polarization index modeling and analysis and cloud-based electronic design automa-

tion algorithms and tools.

Ms. Ma is the recipient of the 2020 and 2021 IEEE Electromagnetic Compatibility Society President's Memorial Award.



Da Li (Member, IEEE) received the B.S. and Ph.D. degrees in electrical engineering from Zhejiang University, Hangzhou, China, in 2014 and 2019, respectively.

From 2017 to 2018, he was a Project Researcher with Nanyang Technological University, Singapore. From 2019 to 2021, he was a Research Fellow with the Science and Technology on Antenna and Microwave Laboratory, Nanjing, China. He is currently an Assistant Professor with Zhejiang University. He has authored or coauthored more than 30 refereed

papers. He was a reviewer of six technical journals and the Technical Program Committee Member of two IEEE conferences. His research interests include machine learning, antennas, matasurfaces, and electromagnetic compatibility.



Er-Ping Li (Fellow, IEEE) received the Diploma in electrical engineering from the Hebei University of Technology, Tianjin, China, in 1983, the M.S. degree in electrical engineering from Xi'an Jiaotong University, Xi'an, China, in 1986, and the Ph.D. degree in electrical engineering from Sheffield Hallam University, Sheffield, U.K., in 1992. He is a Changjiang-Distinguished Professor with the Department of Information Science and Electronic Engineering, Zhejiang University, Hangzhou, China, where he is the Dean of the Joint Institute of Zhejiang University

University of Illinois at Urbana–Champaign. Since 1989, he has been a Research Fellow, a Principal Research Engineer, an Associate Professor, and the Technical Director of the Singapore Research Institute and University. In 2000, he joined the Singapore A*STAR Research Institute of High Performance Computing, Singapore, as a Principal Scientist and the Director. He has authored or coauthored more than 300 papers published in the referred international journals, authored two books published by Wiley/IEEE Press and Cambridge University Press. He holds and has filed a number of patents at the U.S. patent office. His research interests include electrical modeling and design of micro/nanoscale integrated circuits, 3-D electronic package integration, and nanoplasmonic technology.

Prof. Li is the recipient of the 2015 IEEE Richard Stoddart Award on Electromagnetic Compatibility (EMC), the IEEE EMC Technical Achievement Award, the Singapore IES Prestigious Engineering Achievement Award, the Changjiang Chair Professorship Award from the Ministry of Education in China, and a number of Best Paper Awards. He was elected to the IEEE EMC Distinguished Lecturer in 2007. He was an Associate Editor for the IEEE MICROWAVE AND WIRELESS COMPONENTS LETTERS from 2006 to 2008 and a Guest Editor for Special Issues in the IEEE TRANSACTIONS ON ELECTROMAGNETIC COMPATI-BILITY in 2006 and 2010, a Guest Editor for the 2010 IEEE TRANSACTIONS ON MICROWAVE THEORY AND TECHNIQUE Asia-Pacific Microwave Conference Special Issue. He is an Associate Editor for the IEEE TRANSACTIONS ON ELECTROMAGNETIC COMPATIBILITY and the IEEE TRANSACTIONS ON COMPO-NENTS, PACKAGING AND MANUFACTURING TECHNOLOGY. He is the Founding Member of the MTT-8 RF Nanotechnology Committee of the IEEE Microwave Theory and Techniques Society. He is a General Chair and a Technical Chair of many international conferences. He was the President for 2006 International Zurich Symposium on EMC, the Founding General Chair for Asia-Pacific EMC Symposium, and the General Chair for 2008, 2010, 2012, 2016 Asia-Pacific Symposium on Electromagnetic Compatibility and 2010 IEEE Symposium on Electrical Design for Advanced Packaging Systems. He has been invited to give numerous invited talks and plenary speeches at various international conferences and forums. He is a Fellow of the MIT Electromagnetics Academy, USA.



Andreas C. Cangellaris (Life Fellow, IEEE) received the Diploma degree in electrical engineering from the Aristotle University of Thessaloniki, Thessaloniki, Greece, in 1981, and the M.S. and Ph.D. degrees in electrical engineering from the University of California at Berkeley, Berkeley, CA, USA, in 1983 and 1985, respectively.

After a two-year tenure with the Department of Electronics, General Motors Research Laboratories, Detroit, MI, USA, he joined the Department of Electrical and Computer Engineering (ECE), University

of Arizona, Tucson, AZ, USA, initially as an Assistant Professor from 1987 to 1992 and then as an Associate Professor from 1992 to 1997. In 1997, he joined the ECE Department, University of Illinois at Urbana-Champaign, Urbana, IL, USA, as a Full Professor, where he is currently the Vice Chancellor for Academic Affairs and Provost and M.E. Van Valkenburg Professor. He has authored or coauthored more than 250 papers in peer-reviewed journals and conference proceedings on the topics of finite methods for electromagnetic field modeling, multiconductor transmission line modeling, and signal and power integrity of integrated electronic systems. His research group has conducted pioneering work in the advancement of modeling methodologies and computer tools for predictive electromagnetic response performance of the signal and the power distribution networks of integrated electronics at the board, package, and chip levels. Several of the prototype tools developed by his group have been transferred to the microelectronics industry and have contributed to the development of several EDA signal integrity tools. His research interests include applied and computational electromagnetics and its applications to the advancement of modeling methodologies and computer-aided design tools in support of electrical performance analysis and noise-aware design of integrated electronic systems.

Dr. Cangellaris was the Co-Founder of IEEE Topical Meeting on Electrical Performance of Electronic Packaging in 1991. He is an Editor for *IEEE Press Series on Electromagnetic Wave Theory*. He is an Active Member of the IEEE Microwave Theory and Techniques Society (IEEE MTT-S) and the IEEE Components Packaging and Manufacturing Technology Society, contributing to numerous professional activities, conferences, and symposia organized and sponsored by them. From 2010 to 2012, he was a Distinguished Lecturer of the IEEE MTT-S. He was the recipient of the 2000 University of Illinois, ECE Department Outstanding Faculty Teaching Award and the 2005 Alexander von Humboldt Research Award for outstanding contributions to electromagnetic theory.



Xu Chen (Member, IEEE) received the B.S., M.S., and Ph.D. degrees in electrical engineering from the Department of Electrical and Computer Engineering, University of Illinois at Urbana–Champaign, Urbana, IL, USA, in 2005, 2014, and 2018, respectively.

From 2005 to 2012, he was a Hardware Engineer with the IBM Systems Group, Poughkeepsie, NY, USA. In 2013 and 2015, he was with Apple, Cupertino, CA, USA. Since 2018, he has been a Teaching Assistant Professor with the Department of Electrical and Computer Engineering, University of Illinois at

Urbana-Champaign, Urbana, IL, USA. He is a Faculty Member of the Center for Advanced Electronics through Machine Learning, Urbana. His current research interests include stochastic modeling, uncertainty quantification, and machine learning techniques, especially as they apply to electromagnetics and circuit problems.

Dr. Chen was the recipient of the Best Conference Paper Award at IEEE Electrical Design of Advanced Packaging and Systems Symposium in 2017. He was also the recipient of the Raj Mittra Outstanding Research Award, the Mavis Future Faculty Fellowship, and the USNC-URSI Fellowship Grant Award.